Charge transfer dynamics in conjugated polymer/MoS2 organic/2D heterojunctions

Supplementary Information

Charge Transfer Dynamics in Conjugated Polymer/ MoS$_2$ Organic/2D Heterojunctions

Christopher E. Petoukhoff,[1]* Sofiia Kosar,[1] Manami Goto,[1] Ibrahim Bozkurt,[2] Manish Chhowalla,[2] and Keshav M. Dani[1]

1. Femtosecond Spectroscopy Unit, Okinawa Institute of Science and Technology Graduate University, Onna, Okinawa 904-0495, Japan.

2. Department of Materials Science and Engineering, Rutgers University, 607 Taylor Road, Piscataway, New Jersey 08854, United States.
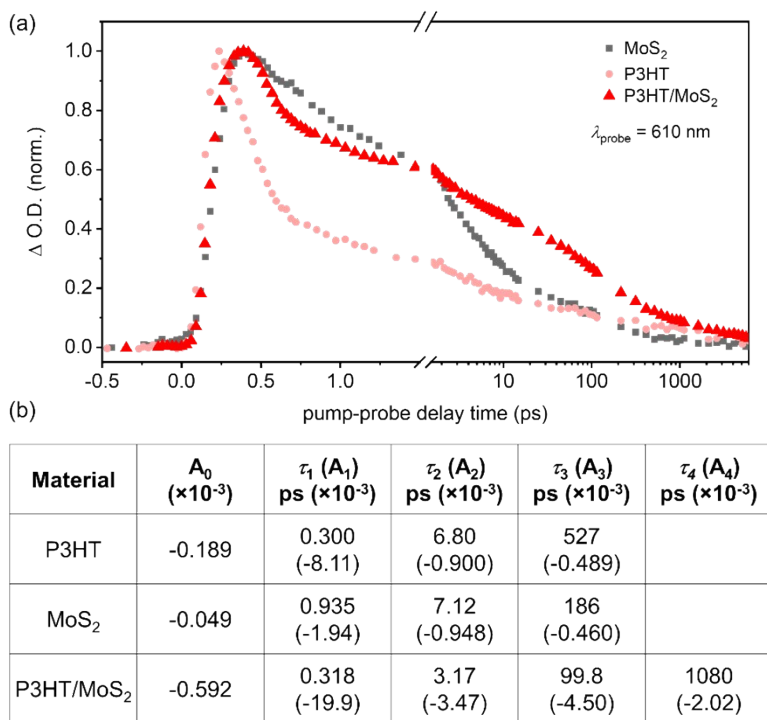
*E-mail: christopher.petoukhoff@oist.jp
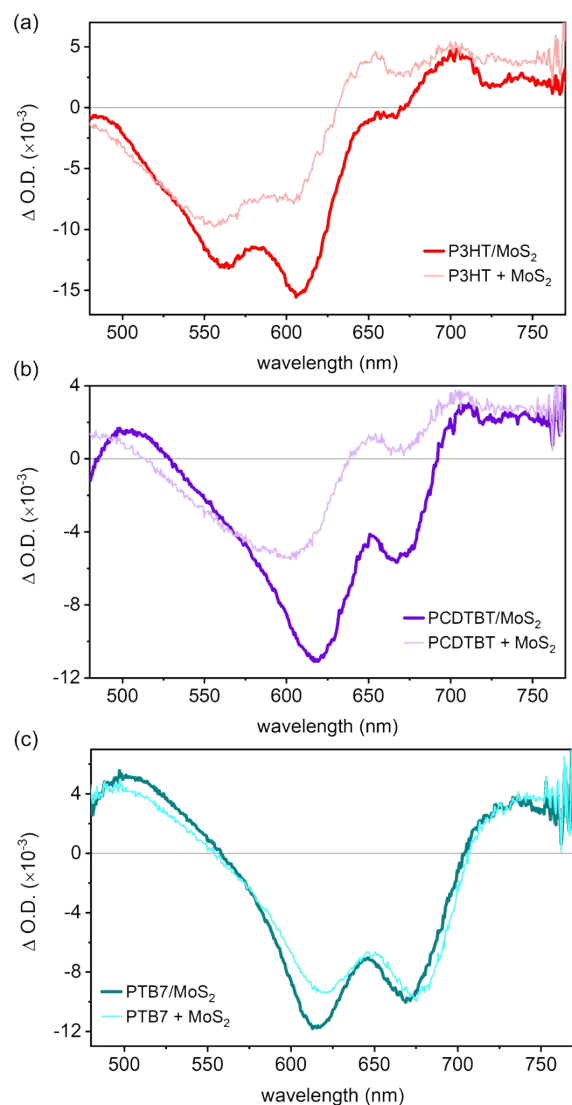
Figure S1. Transient absorption (TA) spectra for all conjugated polymer/MoS$_2$ heterojunctions compared with the TA spectra of the sum of their neat constituents, taken at a pump-probe delay time of 270 fs. Pump wavelength was 660 nm for P3HT and PCDTBT, and 435 nm for PTB7, with a fluence of 61.2 μJ cm^{-2}. From top-to-bottom: (a) P3HT; (b) PCDTBT; and (c) PTB7 heterojunctions.

The TA spectra for all the polymer/MoS$_2$ heterojunctions were not simply a sum of the TA spectra of their individual components (Figure S1). In particular, for all polymer/MoS$_2$ heterojunctions, the bleach signal at ~620 nm, which we attributed to largely arising from MoS$_2$

B- excitons, was increased to the largest degree relative to the signal from the sum of the neat constituents.

(a)

(b)

Material	A_0 $(\times 10^{-3})$	τ_1 (A_1) ps $(\times 10^{-3})$	τ_2 (A_2) ps $(\times 10^{-3})$	τ_3 (A_3) ps $(\times 10^{-3})$	τ_4 (A_4) ps $(\times 10^{-3})$
P3HT	-0.189	0.300 (-8.11)	6.80 (-0.900)	527 (-0.489)	
MoS_2	-0.049	0.935 (-1.94)	7.12 (-0.948)	186 (-0.460)	
$P3HT/MoS_2$	-0.592	0.318 (-19.9)	3.17 (-3.47)	99.8 (-4.50)	1080 (-2.02)

Figure S2. (a) Normalized kinetic traces of $P3HT/MoS_2$ organic/2D heterojunction and its neat constituents for pump wavelength of 660 nm and probe wavelength of 610 nm. (b) Amplitudes and decay times for components used in multi-exponential fits.

We investigated the probe wavelength of 610 nm, corresponding to the B-exciton of MoS_2 as a way to monitor the change in dynamics between the neat films and the $P3HT/MoS_2$ heterojunction. Both $P3HT/MoS_2$ and neat MoS_2 films displayed a rise time of ~200 fs for the bleach signals at 610 nm (Figure S2a), whereas the bleach from neat P3HT film formed instantly (instrument-response-function-limited signal). This suggests that the signal at 610 nm within $P3HT/MoS_2$ had a larger contribution from MoS_2 than P3HT, particularly at early timescales. MoS_2 displayed 3 components to the decay at this wavelength, corresponding to carrier trapping (0.94 ps), exciton-phonon scattering (7.1 ps), and radiative recombination (186 ps; Figure S2)

[Homan, *et al.* Nano Letters, 17, 2017]. Neat P3HT displayed similar decay components, attributed to polaron pair formation (0.3 ps), exciton-exciton annihilation (6.8 ps), and radiative recombination of singlet excitons (527 ps) [Guo *et al.*, J. Am. Chem. Soc., 131, 2009]. After the initial rise, the P3HT/MoS$_2$ signal had a rapid decay of similar timescale (0.3 ps) to the fast decay component in neat P3HT (Figure S2b), corresponding to polaron pair formation. The second and third decay components were faster than either of the neat films (3.2 ps and 99.8 ps, respectively), due to competing effects of exciton-exciton annihilation and exciton-phonon scattering (τ_2) and increased carrier density in the heterojunction (τ_3). P3HT/MoS$_2$ had an additional, long-lived decay component (1.08 ns), which we attribute to charge recombination [Homan, *et al.* Nano Letters, 17, 2017]. This shows that the ground states of MoS$_2$ and P3HT within the heterojunction remained depleted for a much longer timescale than the ground states of the neat constituents.
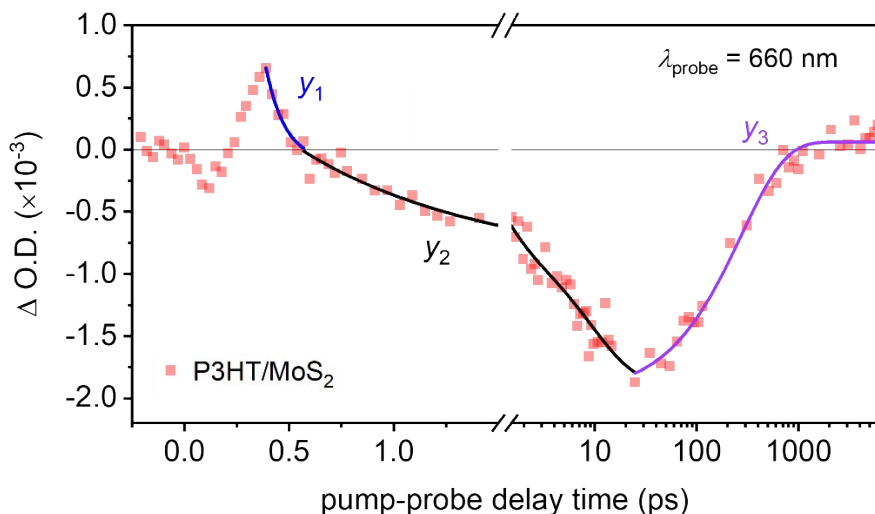
Figure S3. Kinetic trace of P3HT/MoS$_2$ organic-2D heterojunction for pump and probe wavelength of 660 nm. Overlaid are multi-exponential decay (y_1, y_3) and rise (y_2) fits to the curve at different timescales. The decay curves were fit to: $y_{1,3} = A_1 e^{(-t/\tau_1)} + A_0$, and the rise curve was fit to: $y_2 = A_1\left[1-e^{(-t/\tau_1)}\right] + A_2\left[1-e^{(-t/\tau_2)}\right] + A_0$, where t is the pump-probe delay time; A_i are the amplitudes of the different components of the decay/rise; τ_i are the decay/rise constants of the different components; and A_0 is a constant offset for long-lived states.

The signal at 660 nm at early timescales (less than 1 ps) was a convolution of both photoinduced absorption by polaron pairs in P3HT along with the A-exciton bleach of MoS$_2$. After the photoinduced absorption peak, from 390 fs, the signal decayed in < 120 fs (y_1 decay constant was 10 fs, but the instrument response function was 120 fs), suggesting that polaron pairs in P3HT/MoS$_2$ decayed at ultrafast time scales. After 1 ps, the signal showed a rising bleach (y_2) due to charge transfer from the A-exciton of MoS$_2$, with time constants of 725 fs and 9.1 ps. Hence, electron transfer from MoS$_2$ to P3HT polaron pair states occurred within 9.1 ps. The long-time dynamics show the decay of the bleach signal, with a lifetime of 275 ps.
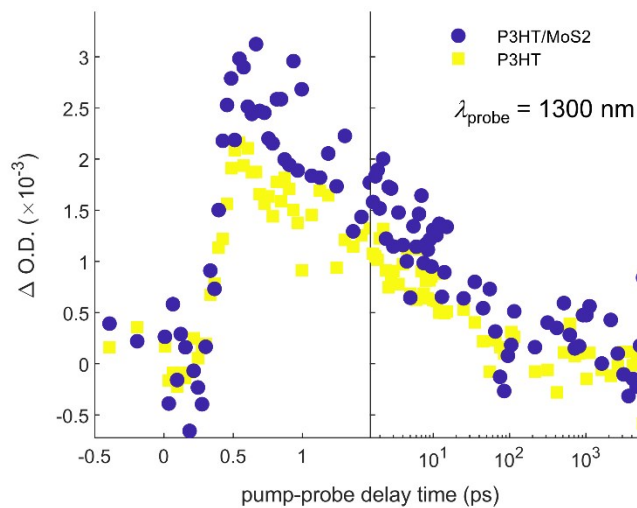
Figure S4. Kinetic trace of P3HT/MoS$_2$ and neat P3HT for pump wavelength of 660 nm and probe wavelength of 1300 nm (*i.e.*, exciton states).

There was only a slight increase in the exciton signal at 1300 nm within P3HT/MoS$_2$, particularly at early timescales (less than 10 ps). However, the changes were small relative to the noise at this wavelength, and so were taken to be negligible.
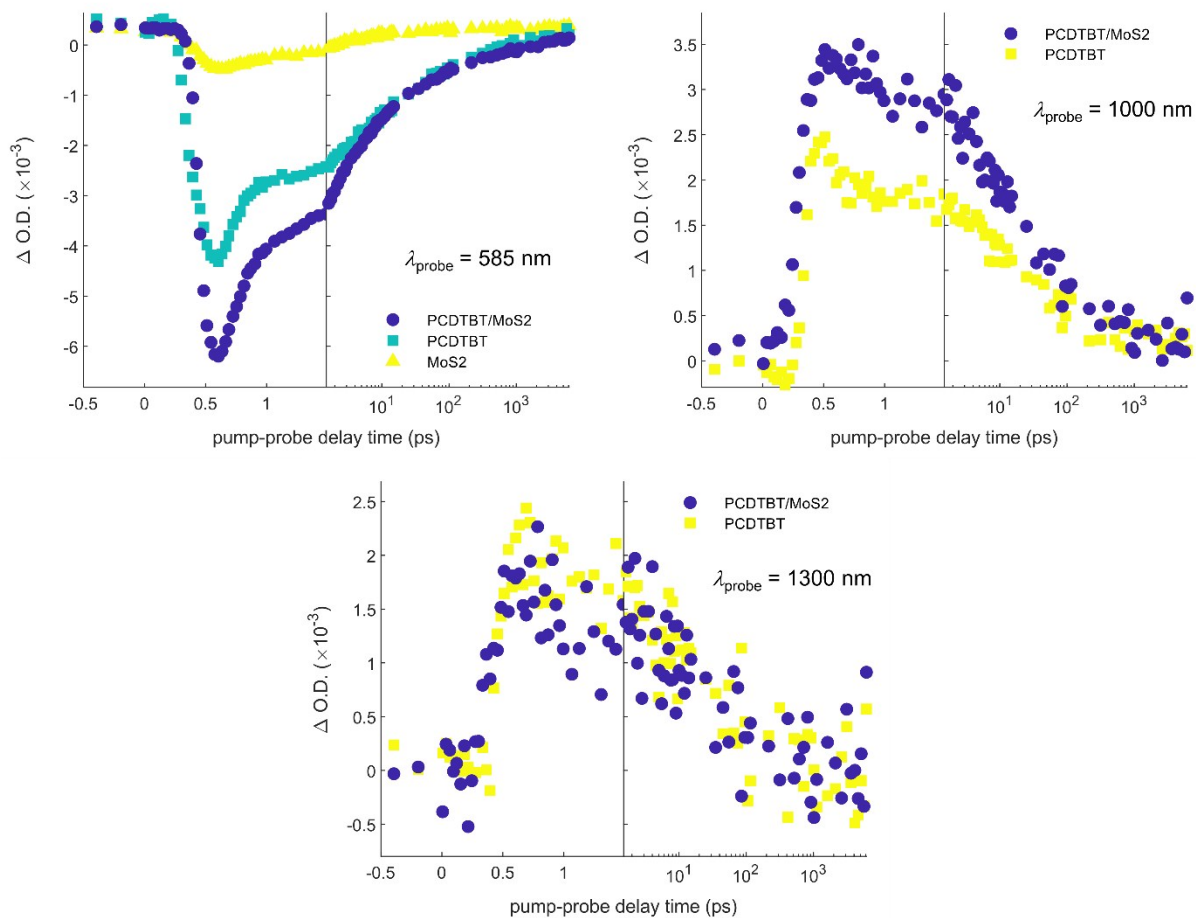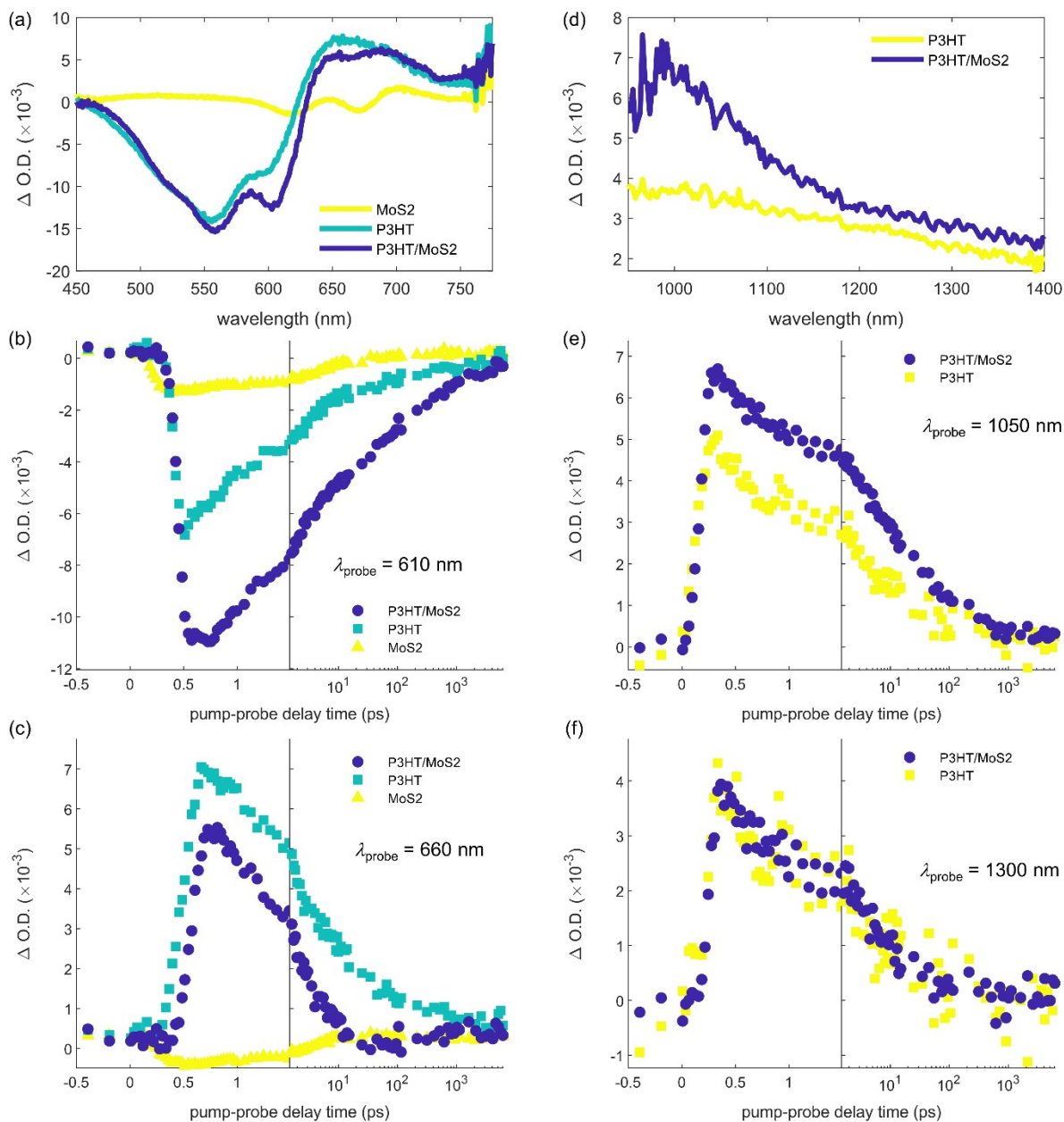
Figure S5. Kinetic traces of PCDTBT/MoS$_2$ heterojunction and its neat constituents for pump wavelength of 660 nm and probe wavelengths of (a) 585 nm; (b) 1000 nm; and (c) 1300 nm.
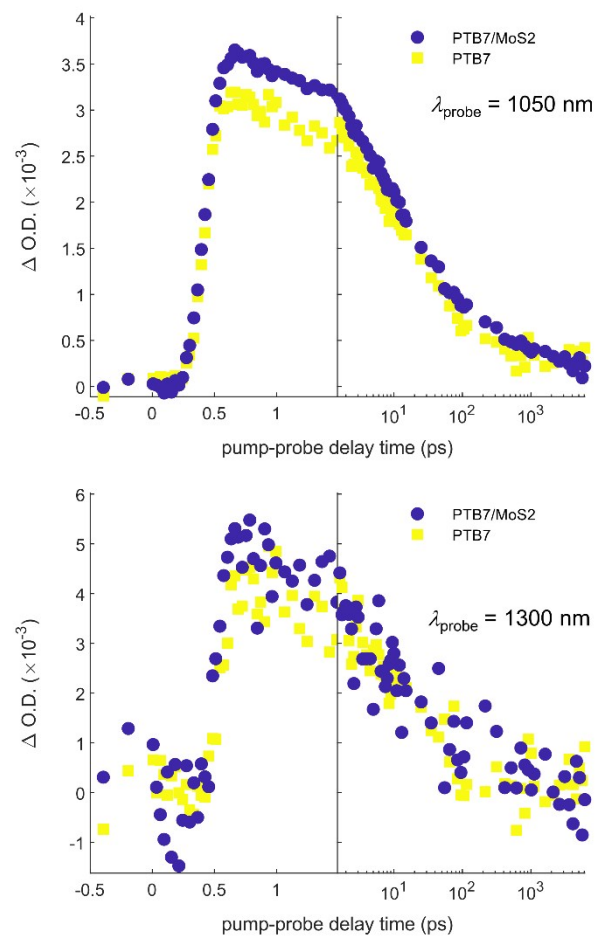
Figure S6. Kinetic traces of PTB7/MoS$_2$ and neat PTB7 for pump wavelength of 435 nm and probe wavelengths of (a) 1050 nm; and (b) 1300 nm.

When selectively pumping the conjugated polymers instead of MoS_2, there was no signature of charge transfer from polymers to MoS_2 (Figures S7-S9). For P3HT/MoS_2 and PCDTBT/MoS_2 (Figures S7 and S8), a pump wavelength of 570 nm was selected to excite predominantly the polymer, while minimizing MoS_2 absorption. However, MoS_2 still had appreciable absorption at this wavelength (Figure 1b). We observed the same general trends for P3HT/MoS_2 and PCDTBT/MoS_2 when exciting at 570 nm that we observed when exciting at 660 nm: increased bleach signal at 620 nm from B-excitons in MoS_2 (Figure S7b and S8b); decreased polaron pair photoinduced absorption signal at 660 nm (Figure S7c and S8c); increased polaron population at ~1000 nm (Figure S7e and S8e); and negligible change in the exciton population at 1300 nm (Figure S7f and S8f). The major difference exciting with 570 nm is that the changes between the polymer/MoS_2 heterojunctions and its neat constituents were significantly less than exciting MoS_2 A-excitons resonantly. This suggests that the same fundamental process occurred when selectively exciting P3HT and PCDTBT due to the small, but appreciable absorption by MoS_2 at this wavelength.
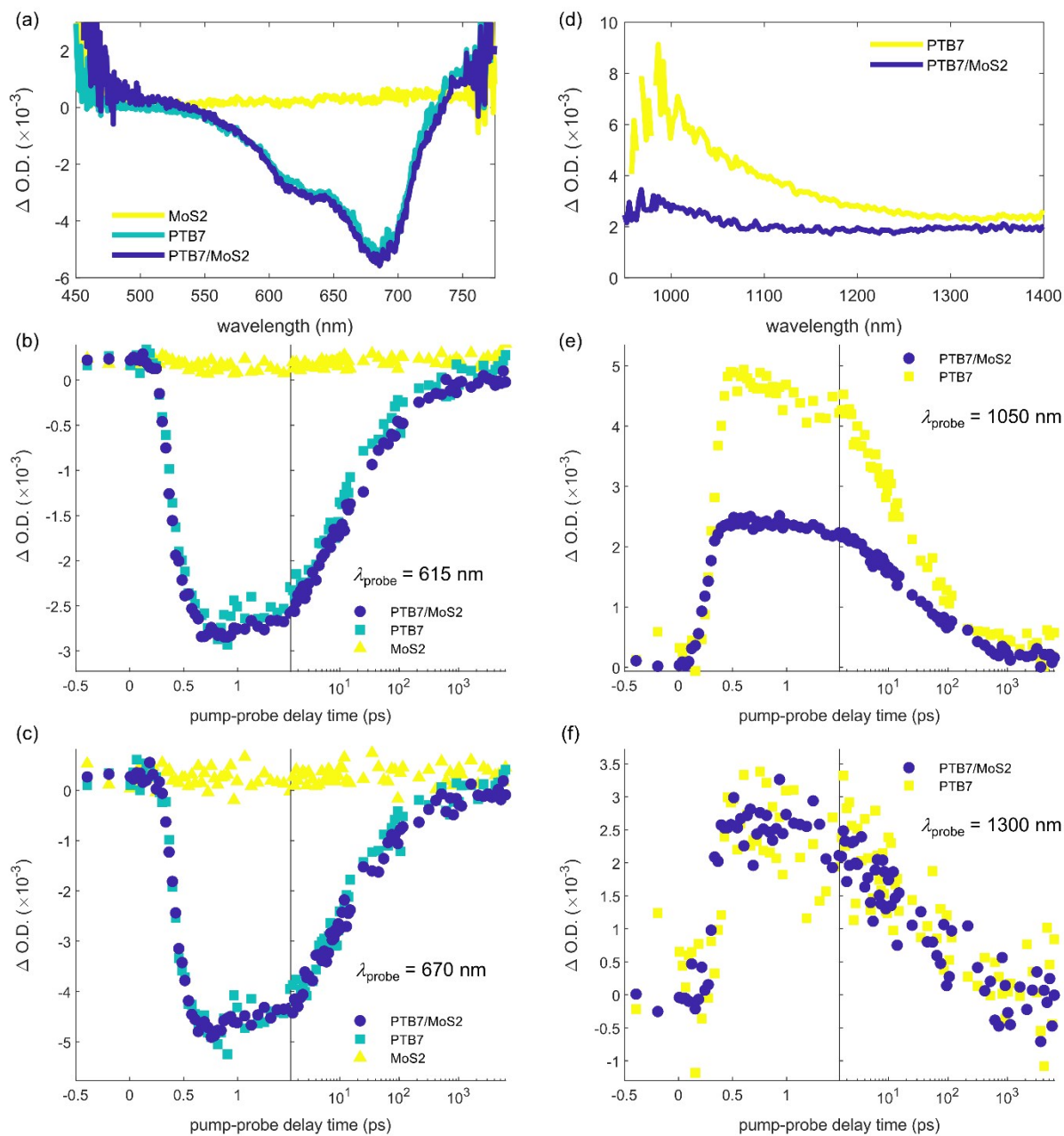
Figure S7. Transient absorption (TA) spectra and kinetic traces for P3HT/MoS$_2$ heterojunction and its neat constituents, with a pump wavelength of 570 nm and fluence of 4.1 μJ cm^{-2}. Visible (a) and near-infrared (d) spectra were taken at a pump-probe delay time of 400 fs. (b,c,e,f) Kinetic traces were extracted from the TA spectra at probe wavelengths of (b) 610 nm; (c) 660 nm; (e) 1050 nm; and (f) 1300 nm.

S10
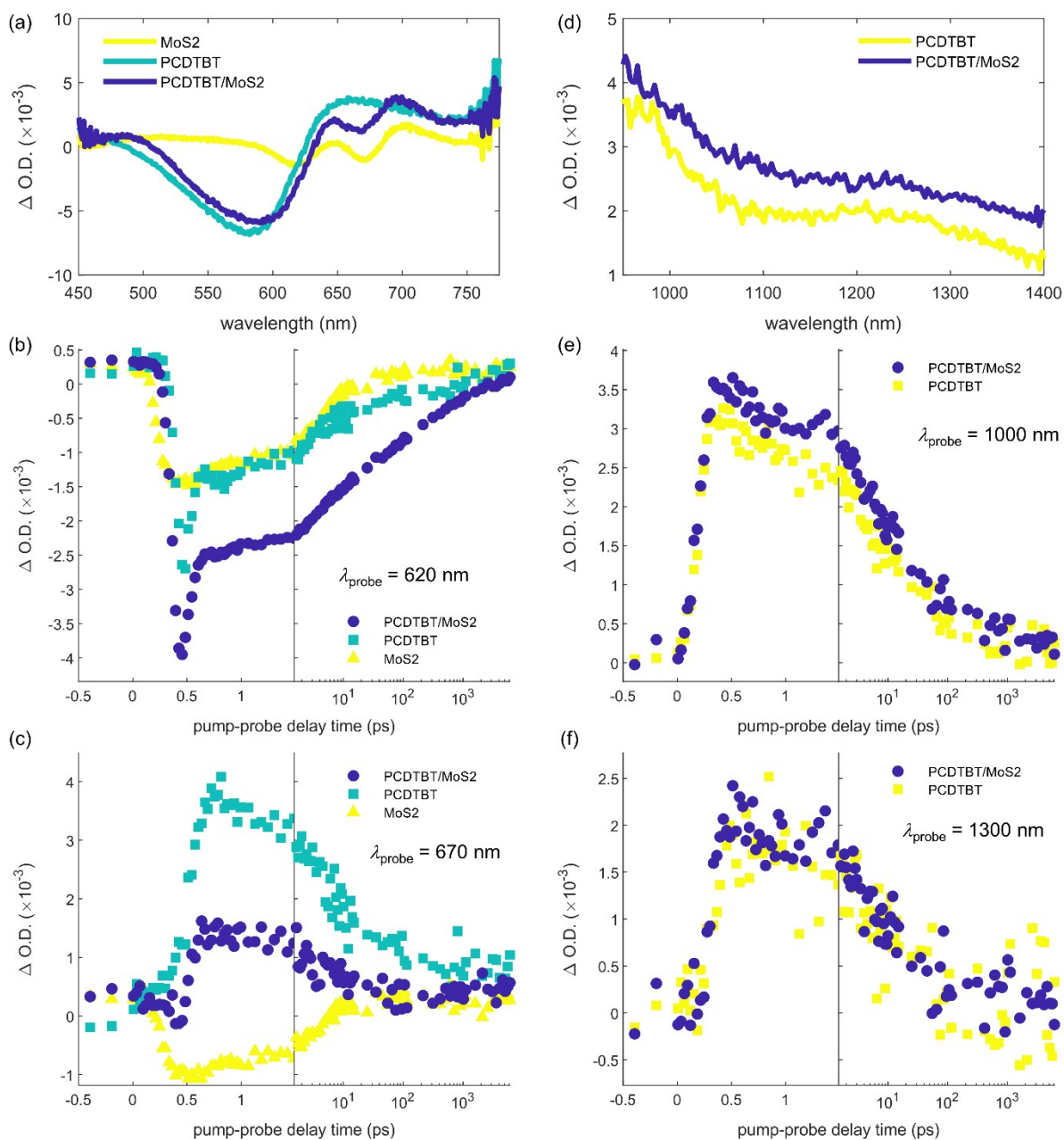
Figure S8. Transient absorption (TA) spectra and kinetic traces for PCDTBT/MoS$_2$ heterojunction and its neat constituents, with a pump wavelength of 570 nm and fluence of 4.1 μJ cm^{-2}. Visible (a) and near-infrared (d) spectra were taken at a pump-probe delay time of 400 fs. (b,c,e,f) Kinetic traces were extracted from the TA spectra at probe wavelengths of (b) 620 nm; (c) 670 nm; (e) 1000 nm; and (f) 1300 nm.

As mentioned in the main text, to avoid exciting MoS_2, we employed the low bandgap polymer, PTB7, allowing us to pump at an energy less than the A-exciton in MoS_2, which is its lowest energy absorption. We selectively excite PTB7 off-resonance at 715 nm to avoid photoexcitations in MoS_2 (Figure 1c). When selectively exciting PTB7, there was no change between the TA spectra or kinetic traces at any visible wavelength with or without MoS_2 (Figure S9a-c). The only difference observed was the polaron signal at 1050 nm, which was reduced by nearly half in PTB7/MoS_2 relative to neat PTB7 (Figure S9d,e), although the exciton signal was again, unaffected (Figure S9f). This was different compared to P3HT/MoS_2 and PCDTBT/MoS_2, which were excited with 570 nm, a wavelength that MoS_2 absorbs. This enabled MoS_2 to transfer electrons to P3HT and PCDTBT, though to a lesser extent than when pumped on resonance. Since PTB7/MoS_2 was pumped at 715 nm, there was no absorption by MoS_2, and thus no electron transfer to PTB7. Because there was no change in signal from MoS_2 in any part of the spectrum, we concluded that there was no charge transfer from PTB7 to MoS_2.

Figure S9. Transient absorption (TA) spectra and kinetic traces for PTB7/MoS$_2$ heterojunction and its neat constituents, with a pump wavelength of 715 nm and fluence of 4.1 μJ cm^{-2}. Visible (a) and near-infrared (d) spectra were taken at a pump-probe delay time of 400 fs. (b,c,e,f) Kinetic traces were extracted from the TA spectra at probe wavelengths of (b) 615 nm; (c) 670 nm; (e) 1050 nm; and (f) 1300 nm.

Table S1. Decay constants and amplitudes obtained from multi-exponential fits to Δ O.D. kinetic traces of polaron states for the different neat conjugated polymer films and polymer/MoS$_2$ heterojunctions. Pump wavelength was 660 nm for P3HT and PCDTBT samples or 435 nm PTB7 samples; probe wavelength was ~1000 nm. Each kinetic trace was fit to two or more exponential decays using the general equation: Δ O.D. $= A_{\text{fast}}e^{(-t/\tau_{\text{fast}})} + A_1 e^{(-t/\tau_1)} + A_2 e^{(-t/\tau_2)} + A_3 e^{(-t/\tau_3)} + A_0$, where t is the pump-probe delay time; A_i are the amplitudes of the different components of the decay; τ_i are the decay constants of the components of the decay; A_0 is a constant offset for long-lived polarons; and A_{fast} and τ_{fast} are the amplitudes and decay constants of the fast (few hundred fs) components of the decay of neat P3HT and PCDTBT.

| Sample	τ_{fast}, ps ($A_{\text{fast}} \times 10^{-3}$)	τ_1, ps ($A_1 \times 10^{-3}$)	τ_2, ps ($A_2 \times 10^{-3}$)	τ_3, ps ($A_3 \times 10^{-3}$)	$A_0 \times 10^{-3}$
P3HT	0.229 ± 0.0262 (2.57 ± 0.270)	3.80 ± 0.588 (1.03 ± 0.0528)	72.5 ± 9.09 (0.827 ± 0.0567)	--	0.0556 ± 0.0148
P3HT/MoS$_2$	--	35.6 ± 3.83 (2.74 ± 0.152)	562 ± 139 (1.15 ± 0.155)	--	0.124 ± 0.0532
PCDTBT	0.238 ± 0.0640 (4.03 ± 2.02)	7.37 ± 2.58 (0.835 ± 0.143)	104 ± 30.4 (0.918 ± 0.161)	--	0.233 ± 0.0283
PCDTBT/MoS$_2$	--	3.08 ± 0.653 (1.44 ± 0.102)	74.6 ± 10.9 (1.74 ± 0.113)	--	0.316 ± 0.0408
PTB7	--	2.63 ± 0.344 (1.42 ± 0.0651)	56.8 ± 4.44 (1.84 ± 0.0631)	--	0.353 ± 0.0226
PTB7/MoS$_2$	--	1.62 ± 0.152 (1.51 ± 0.0617)	23.7 ± 2.16 (1.76 ± 0.0521)	560 ± 66.8 (0.766 ± 0.0439)	0.259 ± 0.0187
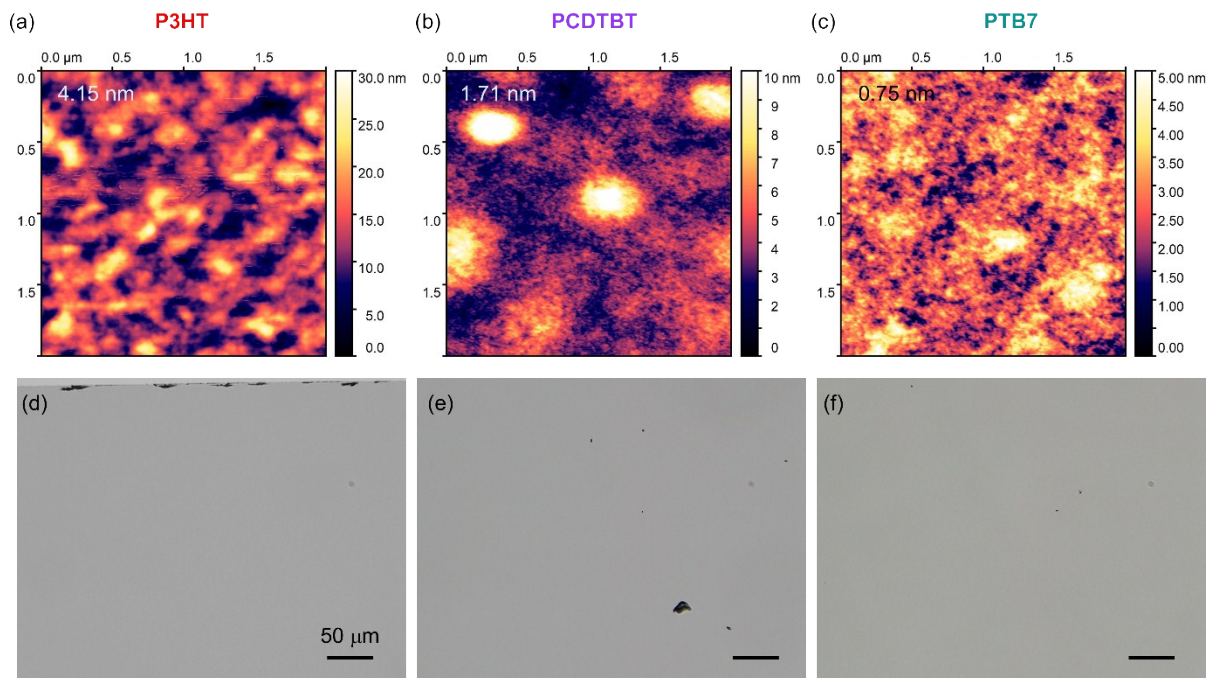
Figure S10. Atomic force microscopy (AFM) (a-c) and optical (d-f) images of neat polymer films: (a,d) P3HT; (b,e) PCDTBT; (c,f) PTB7. The root-mean-square (RMS) surface roughness is shown in the top left corner of each AFM image. Scale bars in d-f are all 50 μm.

The optical images of the polymer films show that the films were uniform over large areas (10s – 100s of μm). The polymer films exhibited lateral features on both the tens of nanometer scale (10-30 nm, 30-50 nm, and 15-30 nm for P3HT, PCDTBT, and PTB7, respectively) as well as on the hundreds of nanometer scale (100-200 nm for P3HT and ~300 nm for PCDTBT and PTB7). Each film had only few nanometer or less root-mean-square surface roughness (4.15 nm, 1.71 nm, and 0.75 nm for P3HT, PCDTBT, and PTB7). This films in general were similar, with none of the films exhibiting any nanoscale structural ordering.
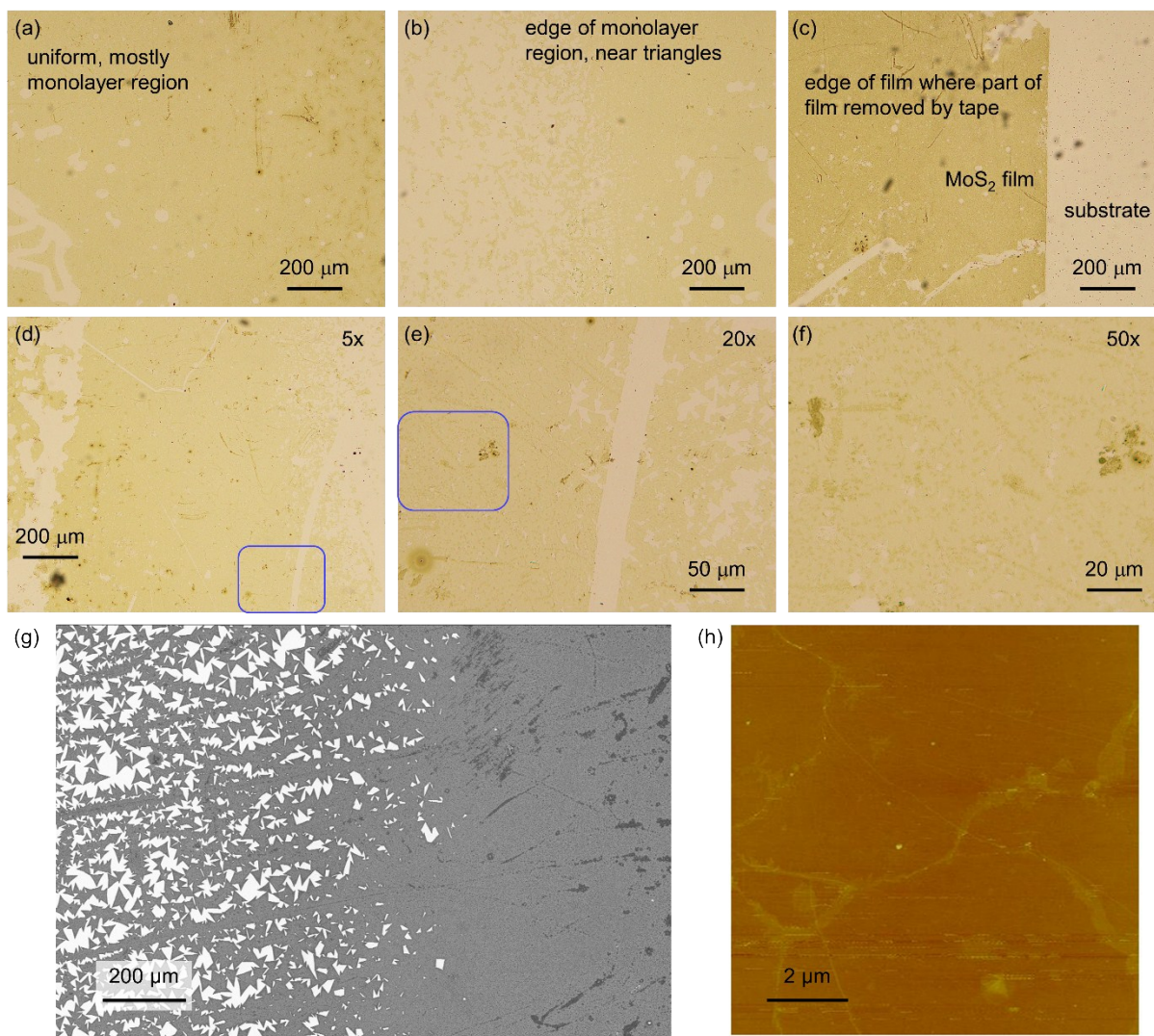
Figure S11. Optical transmission images of CVD-grown MoS$_2$ films transferred from SiO$_2$/Si substrates onto fused silica using thermal release tape method. (a-c) Different region types demonstrating efficiency of transfer process: (a) Typical, uniform, mostly monolayer region towards centre of the film; (b) region towards edge of continuous monolayer film, where isolated traingles can be observed; (c) region near edge of taped film, showing the well-defined edge from lifting off the film using tape. (d-f) Typical uniform region used for measurements. (d) Low magnification image of region. Blue box is the region magnified to 20× in (e); blue box in (e) is the region magnified to 50× in (f). (g) Scanning electron microscope (SEM) image of MoS$_2$ film, taken near the edge of the monolayer film, near the isolated triangles. (h) AFM image of MoS$_2$ film from a predominantly monolayer region, where the grain boundaries can be observed.
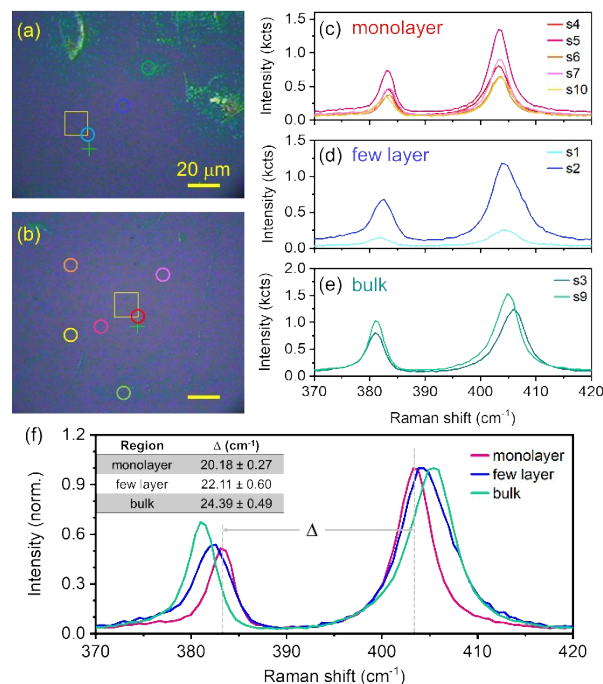
Figure S12. Raman spectra of MoS_2 film taken from 2 different regions: (a) near the bulk, and (b) near the uniform regions of the film. (c-e) Individual spectra taken from different regions in the film, where the colours of the spectra match the circles in (a,b). The spectra were grouped into those taken from: (c) monolayer; (d) few layer; and (e) bulk regions based on the splitting between the two modes (A_{1g} and E_{2g}^1), Δ. (f) Averaged spectra (normalized to A_{1g} peak) from each of the different regions. The splitting values are shown for each of the different regions: monolayer-thick regions are characterized by splitting values around 20 cm^{-1} or less, few-layer thick regions are characterized by splitting values between 20 cm^{-1} and 24 cm^{-1}, and bulk regions are characterized by regions >24 cm^{-1} [Lee *et al.*, ACS Nano, 4 (5), 2010, 2695-2700].
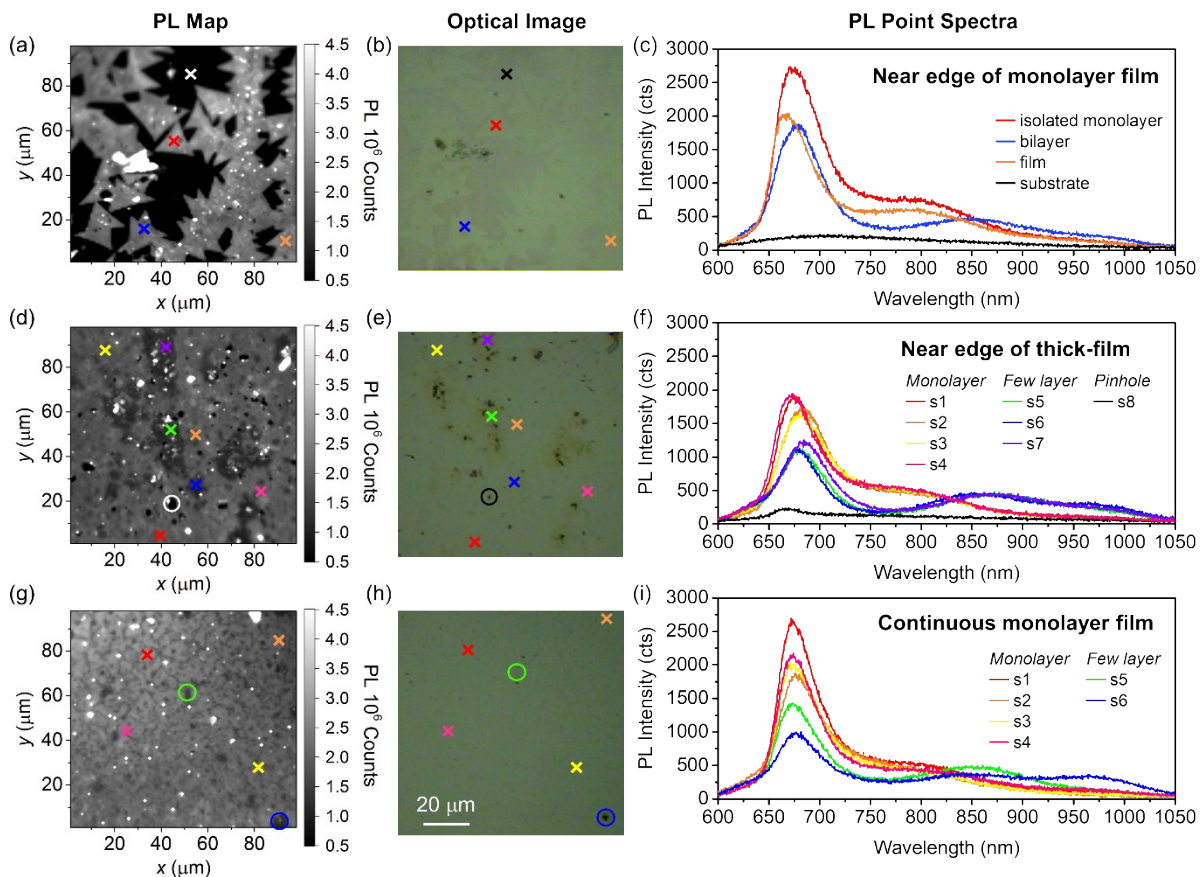
Figure S13. Photoluminescence (PL) maps (a,d,g) with corresponding optical images (b,e,h) and point spectra (c,f,i) from different regions of an MoS$_2$ film: (a-c) near the edge of the film, close to the monolayer triangles; (d-f) near the edge of the thick-film, close to the bulk; (g-i) within the continuous monolayer portion of the film. (a-c) Shows clearly the differences in PL between an isolated monolayer, a bilayer, and the continous film, with the bilayer having a pronounced peak at ~860 nm corresponding to the indirect bandgap, and overall reduced intensity of the PL. (d-f) Shows the PL from predominantly bulk or few layer regions, where, again, the longer wavelength peaks at ~860 nm and ~980 nm are pronounced, and the main peak ~675 nm is reduced. (g-i) Characteristic PL from regions of the continuous monolayer film, where measurements were taken. Note that although there were still some few-layer regions, the film was predominantly monolayer.